# Experimental Evaluation of Differential Chip-to-Antenna Bondwire Interconnects above 110 GHz

Václav Valenta, Hermann Schumacher, Thomas Spreng, Volker Ziegler, Dragos Dancila, Anders Rydberg

# Experimental Evaluation of Differential Chip-to-Antenna Bondwire Interconnects above 110 GHz

Václav Valenta and Hermann Schumacher
Institute of Electron Devices and Circuits, Ulm University
89081Ulm, Germany
vaclav.valenta@ieee.org

Thomas Spreng, Volker Ziegler
Airbus Group Innovations
81663 Munich, Germany

Dragos Dancila, Anders Rydberg
Angstrom Laboratory, Uppsala University
75121 Uppsala, Sweden

***Abstract*—Bondwire interconnects for differential chip-to-antenna interfaces are investigated. Two different compensation structures for different interconnect lengths are designed and evaluated using dedicated transmit and receive BiCMOS modules operating across a 110 to 156 GHz band. Measurement results demonstrate that a 9 GHz bandwidth and a minimum insertion loss of 0.2 dB can be achieved for interconnects as long as 0.8 mm, showing that the well established wire-bonding techniques are still an attractive solution even beyond 100 GHz. Reproducibility of the proposed solution is assessed as well.**

***Keywords—wire-bonding, bondwire interconnect, MMIC.***

## I. Introduction

On-chip antennas fully integrated in standard BiCMOS processes become a reality in emerging mm-wave and THz imaging and radar systems [1]-[4]. This success is possible thanks to fast and accurate EM computational methods and advanced wafer processing techniques that allow localized backside wafer etching or precise wafer thinning to reduce losses in low-resistivity silicon substrates [5]. Although fully integrated on-chip antennas significantly facilitate packaging and offer good radiation properties already today, the relatively large area they occupy on-chip (half wavelength in the air above 100 GHz is less than one and half millimeter) may still be prohibitive for future low-cost millimeter-wave imaging and radar systems deploying a large number of transmit/receive (TX/RX) channels. Moreover, to achieve good radiation properties, the space surrounding the on-chip radiating elements shouldn't contain any metal fillers, which is often incompatible with standard high-volume integration processes that require specified metal densities across all layers to achieve high yield.

Off-chip antennas, on the other hand, offer ease of manufacturing at lower costs and superior performance namely in terms of radiation efficiency and bandwidth compared to their on-chip counterparts [6]. At the same time, bondwire interconnection techniques are widespread and very popular due to the rather simple technology involved. Performance degradation of chip-to-antenna interconnects at higher frequencies has been, however, identified as one of the key challenges due to reactive discontinuity introduced by the bondwire. Nonetheless, several studies have shown that bondwire interconnects with excellent properties in the mm-wave range are possible and reproducible [9]-[11]. Flip-chip interconnects are another alternative, however, the overall complexity of the mounting process and other inherent drawbacks of this technique such as dielectric detuning by the opposite substrate [7], [8], lack of direct visual control or worse heat sinking make this solution less attractive for mm-wave interconnects. As a result, bondwire interconnects are in certain systems inevitable and therefore need to be carefully assessed. The latter is also the main focus of this paper, which presents results of an experimental study on two different bondwire interconnects proposed for mm-wave systems operating above 110 GHz.

## II. Chip-to-Antenna Interconnect Structures

Two different types of chip-to-antenna bondwire interconnects were evaluated using two dedicated pairs of TX and RX boards equipped with identical ICs that use Gilbert cell multipliers to get the LO reference signal to the F-band [13]. A block diagram of these modules with different

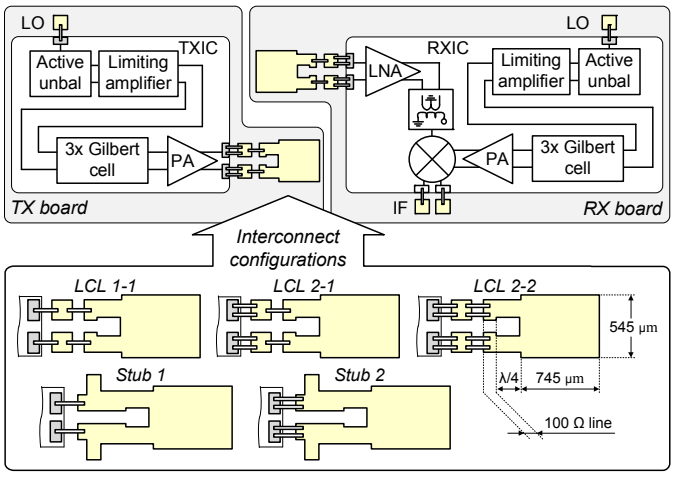


Fig. 1. A block diagram of the TX and RX modules used for evaluation of different configurations of bondwire interconnects.

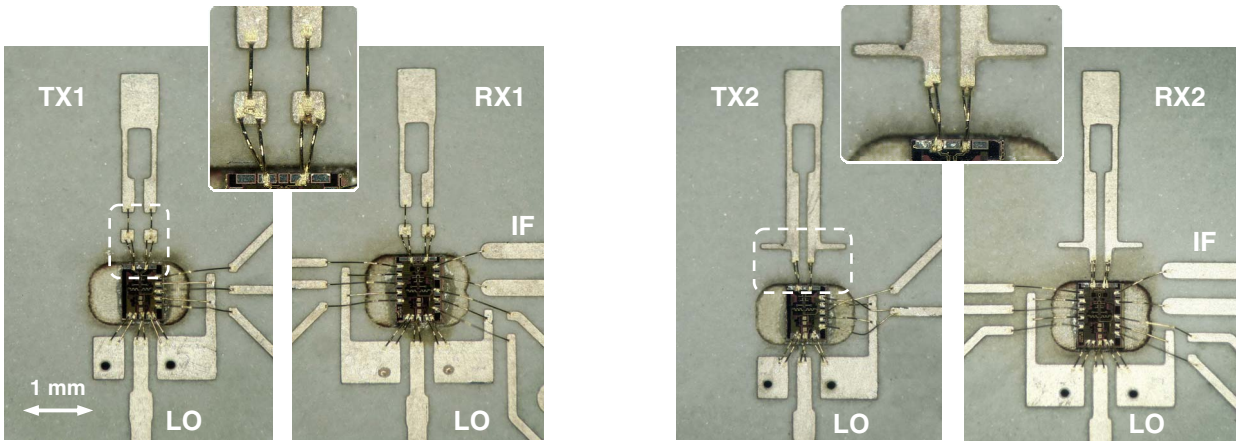


Fig. 2. A photograph of two pairs of realized TX and RX modules with two different bondwire compensating structures: LCL network (left figure, configuration LCL 2-1) and microstrip stub network (right figure, configuration Stub 2).

configurations of the differential chip-to-antenna interconnect is depicted in Fig. 1. A photograph is shown in Fig. 2. Beside the inherent immunity to common-mode noise, cancelation of even-harmonics or ease of packaging due to the virtual ground, yet another benefit of the differential operation is that the inductive effects of the bondwire are significantly reduced due to the resulting symmetry plane that increases the mutual inductance [12], [14].

### *A. Differential end-fire patch antenna*

A differential end-fire patch antenna has been designed in CST and realized on a 127 µm thick RO3003 substrate. The size of the patch is 745 x 545 µm and its feed-point is matched to a 100 Ω differential line using a quarter-wave transformer, which consists of two 100 µm wide microstrip lines spaced by 300 µm. The simulated return loss and gain of the antenna across the required band are better than -10 dB and 6.9 dBi, respectively. The simulated radiation efficiency is 96%.

### *B. LCL interconnect*

As depicted in Fig. 1 and Fig. 2, the first type of interconnect consists of two bondwire bridges (gold wires with a diameter of 17 µm) with a common contact point at an intermediate off-chip pad that acts as a capacitance of 15 fF. This configuration creates an L-C-L T-network, which turns this interconnect into a resonant structure between the output pads of the IC and the differential feed-point of the antenna. The distance between the output pads of the chip and the antenna structure is 800 µm. The estimated bondwire length at both sides of the T-network is approximately 320 µm. Very low-profile interconnects were possible thanks to the ultrasonic wedge-bonding technique and horizontal alignment of the chip pads and the off-chip metal structures. To further lower the inductance, two bondwires are used in parallel. This configuration was also simulated and the results are depicted in Fig. 3, showing the impedance seen at the interface between the LCL interconnect and the antenna with the quarter-wave transformer for different values of the bondwire inductance across 110-150 GHz band. This figure suggests that bondwire inductance close to 0.25 nH and above might lead to significant mismatch and hence, dual wire-bonding or ribbons should be used.

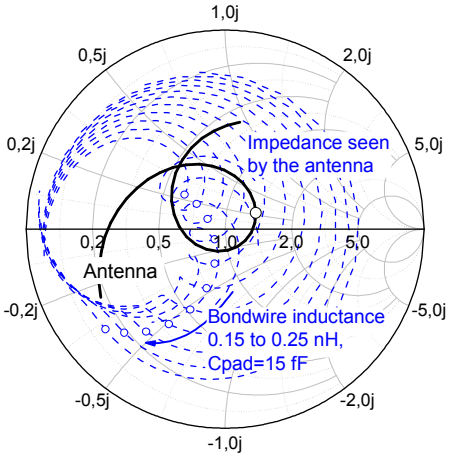


Fig. 3. Matching strategy of the LCL interconnect depicting the impedance at the antenna reference plane. The blue dashed lines show the impedance across 110-150 GHz band seen by the patch antenna for different values of the bondwire inductance. Circles highlight the mid-band (130 GHz).

### *C. Interconnect with differential stubs*

Bondwires in the second topology connect the output chip pads directly to a differential matching structure. The matching structure uses differential stubs to match the chip output together with the bondwire inductance to a 100 Ω differential line. A 500 µm long 100 Ω differential line with 100 µm slot is used to connect the antenna to the matching structure. The whole planar structure was EM simulated and optimized in CST. The distance between the output pads of the chip and the compensation structure is 350 µm and the estimated length of the bondwire is 365 µm. As in the previous case, the influence of the bondwire inductance was estimated using a simple lumped element model together with the EM model of the planar compensation structure and the patch antenna. Simulation results of the impedance at the reference plane of the antenna for bondwire inductance varying from 0.15 to 0.25 nH are depicted in Fig. 4. Compared to the LCL matching network, the simulation results suggest that lower sensitivity to the variation of the bondwire inductance can be expected. The latter has been confirmed by measurements.

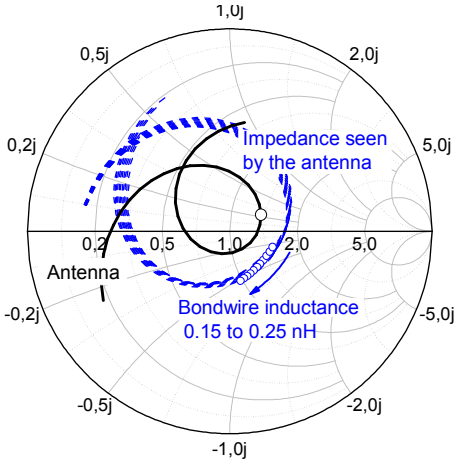


Fig. 4. Matching strategy of the stub interconnect. As in the previous figure, matching across 110-150 GHz at the antenna reference plane is shown for different values of the bondwire inductance.

## III. Experimental Evaluation

### A. Measurement setup

The influence of all bondwire interconnect configurations (LCL 1-1, 2-1, 2-2 and Stub 1, 2 as depicted in Fig. 1) has been evaluated with the help of an experimental 0.5 m long wireless link deploying the realized TX/RX modules. To determine the power applied to the interconnect of the TX module, three different samples of TX ICs were first characterized on-wafer using a waveguide F-band GSG probe connected to a spectrum analyzer via an F-band harmonic mixer extension [13]. Results of the frequency response are depicted in the upper plot of Fig. 5. The maximum output power of 3 dBm (6 dBm differential) was measured at the frequency of 124 GHz. The 3-dB bandwidth is 20 GHz. Results above 140 GHz are illustrated by simulation. The conversion gain of the RX IC was determined based on on-wafer measurements of LNA which was also designed as a separate chip and simulation results of the designed down-converting mixer with an IF buffer. Afterwards, diced chips were glued to cavities in the PCB and bonded to the dedicated on-board compensation structures.

### B. Measurement results

In the next step, a wireless link was established: two LO signals from independent signal generators were fed to the TX/RX modules. The frequency of the LO reference sources was shifted by 1 MHz with respect to each other and simultaneously tuned from 13.75 GHz to 19.5 GHz (which corresponds to 110-156 GHz at the wireless interface) while monitoring the 8 MHz IF at the RX output using a spectrum analyzer. Single-ended measurement results of the IF power detected at one of the differential RX outputs for five different configurations of the bondwire interconnect are depicted in the second plot of Fig. 5. It can be seen that compared to the LCL interconnect, the interconnect with microstrip stubs is more broadband and less susceptible to the changes of the bondwire inductance. For instance, the effect of doubling the bondwire in the stub matching network is not noticeable above 125 GHz. The main improvement of up to 7 dB is observable

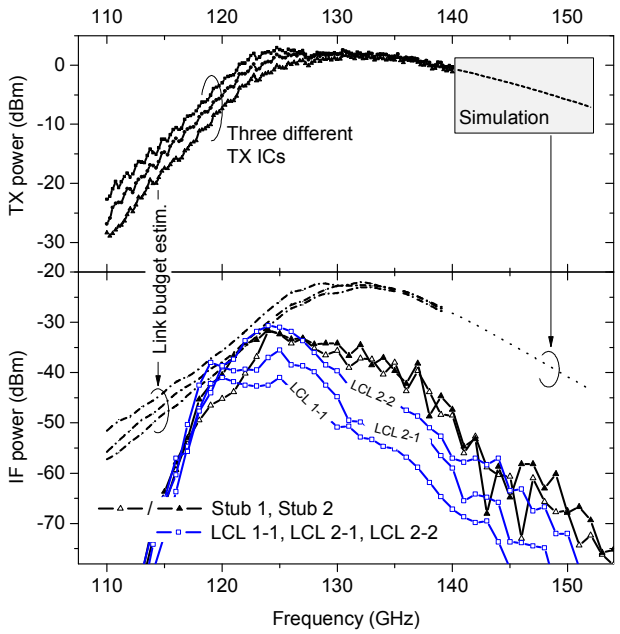


Fig. 5. Single-ended output power of three different TX ICs measured on-wafer and corresponding single ended IF power detected by the RX module with different interconnects at a 0.5 m distance. Link budget estimation curves do not consider losses introduced by the bondwire interconnects.

only in the 117-125 GHz range. The LCL interconnect, on the other hand, clearly shows the importance of the double bonding technique which can improve the link budget by up to 13 dB (LCL 1-1 vs. LCL 2-2 at 125 GHz). The latter observations are also in a good agreement with the simulation results of both types of bondwire interconnect summarized in the previous section. The influence of both matching structures on the overall radiation pattern of realized modules was investigated as well. While the LCL interconnect doesn't introduce any measurable influence, the matching network with differential stubs introduces a local minimum perpendicular to the antenna plane and splits the original single-lobe pattern into two secondary lobes. For this reason, TX/RX modules had to be tilted down towards the maximum during the measurements. This effect has also been observed in simulation results of far-field radiation of the whole off-chip structure.

For comparison, the second plot in Fig. 5 is also showing the estimated IF power derived from the measured TX output power, LNA gain and from the simulated antenna gain, pathloss and conversion gain of RX mixer and IF buffer. Since this estimation doesn't account for losses caused by the chip-to-antenna interconnects in the TX and RX modules, these losses are directly reflected in the difference between the measured and the estimated IF power. Therefore, one half of this difference represents the loss per interconnect at each module and is plotted in Fig. 6 for both LCL and stub interconnecting structures with double bonding. The frequency response above 140 GHz is highlighted as a "simulation" because the TX power was not measured in this band and the link budget equation accounted for the simulated results. The 3-dB bandwidth of both types of interconnect is close to 9 GHz (117.2-126.3 GHz and 117.7-126.6 GHz for the Stub and LCL interconnects, respectively). To determine the

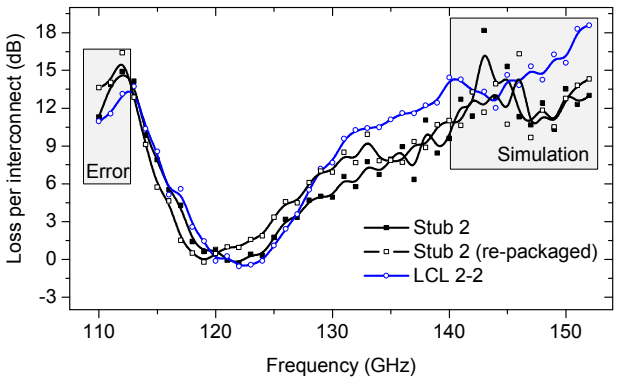


Fig. 6. Loss per interconnect for both compensation topologies derived from the IF measurement results. Measurements of completely re-packaged TX/RX modules with Stub 2 interconnects are depicted as well.

precise value of the minimum insertion loss, exact values of the variables in the link budget equation would need to be known. As a result, the minimum insertion loss is estimated using a lumped element model, which suggests the minimum insertion loss of 0.2 dB and 0.5 dB for the LCL and stub interconnects, respectively.

To evaluate the repeatability of the packaging and bonding procedures, new TX/RX ICs were re-packaged into the modules with the differential stub interconnects and re-bonded using double bonding. The derived loss per interconnect of the second TX/RX prototype is depicted in Fig. 6. Compared to the losses derived in the first prototype, the frequency response exhibits slightly narrower bandwidth and a shift of 1.5-2 GHz towards the lower frequencies. Considering the frequency of operation, various types of measurement errors and inaccuracies during the packaging and bonding procedures, this shift is considered insignificant and proves that this interconnect solution can be expected to be highly repeatable.

## IV. Conclusion

Two different compensation structures suitable for low-cost mm-wave chip-to-antenna bondwire interconnects were presented together with measurement results of an experimental wireless system that operates above 110 GHz and relies on the proposed interconnects. It has been shown that a 7.5% bandwidth and an insertion loss as low as 0.2 dB are possible in this frequency range. In comparison with other recent studies on bondwire interconnects, the bandwidth of the proposed interconnect is rather moderate. However, considering the material used, the operating frequency and namely the overall length of the second proposed interconnect (LCL connection with the overall length of 800 µm), these results are the best reported to date. It has also been demonstrated that the interconnection based on differential microstrip stubs is less sensitive to variations of the bondwire inductance and provides lower losses beyond the 3-dB bandwidth. On the other hand, the undesired shaping of the main radiation lobe due to secondary radiation of the matching stubs is the main remaining challenge that needs to be resolved on the way towards reliable and high-performance mm-wave interconnects. This undesired effect could be avoided, e.g. by using a triplate or inverted microstrip structure at the expense of increased PCB complexity.

Although only one pair of the TX/RX modules was re-packaged, re-bonded and re-measured to prove that this approach to bondwire interconnects can be repeated, it is expected that high reproducibility of the proposed solution can be achieved. Conclusive proof of repeatability of the proposed solution is a remaining task.

## Acknowledgment

This work has been carried out in the framework of the European project NANOTEC (Grant Agreement N°288531).

## References

[1] R. Wang, Y. Sun, M. Kaynak, S. Beer, J. Borngraber, C. J. Scheytt, "A micromachined double-dipole antenna for 122-140 GHz applications based on a SiGe BiCMOS technology," IEEE MTT-S International Microwave Symposium Digest (IMS), Montreal, Canada, June 2012.

[2] E. Ojefors, U. R. Pfeiffer, "A 650GHz SiGe receiver front-end for terahertz imaging arrays," IEEE International Solid-State Circuits Conference (ISSCC), San Francisco, CA, USA, February 2010.

[3] S. Yuan, H. Schumacher, "56 GHz Bandwidth FMCW Radar Sensor with On-Chip Antennas in SiGe BiCMOS," IEEE MTT-S International Microwave Symposium (IMS), Tampa, FL, USA, June 2014.

[4] C. Zhiming, C.-C. Wang, H.-C. Yao, P. Heydari, "A BiCMOS W-Band 2×2 Focal-Plane Array With On-Chip Antenna," IEEE Journal of Solid-State Circuits, vol. 47, no. 10, pp. 2355-2371, Oct. 2012.

[5] F. Korndorfer, M. Kaynak, V. Mu□hlhaus, "Simulation and measurement of back side etched inductors," European Microwave Integrated Circuits Conference (EuMIC), Paris, France, Sept. 2010.

[6] Y. P. Zhang, D. Liu, "Antenna-on-Chip and Antenna-in-Package Solutions to Highly Integrated Millimeter-Wave Devices for Wireless Communications," IEEE Transactions on Antennas and Propagation, vol. 57, no. 10, pp. 2830-2841, Oct. 2009.

[7] T. Krems, W. Haydl, H. Massler and J. Rudiger, "Millimeter-Wave Performance of Chip Interconnections using Wire Bonding and Flip Chip," IEEE MTT-S International Microwave Symposium Digest (IMS), San Francisco, CA, USA, 1996.

[8] A. Jentzsch, W. Heinrich, "Theory and measurements of flip-chip interconnects for frequencies up to 100 GHz," IEEE Transactions on Microwave Theory and Techniques, vol. 49, pp. 871-878, May 2001.

[9] G. Liu, A. Trasser, A. C. Ulusoy, H. Schumacher, "Low-loss, low-cost, IC-to-board bondwire interconnects for millimeter-wave applications," IEEE MTT-S International Microwave Symposium Digest (IMS), Baltimore, MD, USA, June 2011.

[10] S. Beer, H. Gulan, C. Rusch, T. Zwick, "Coplanar 122-GHz Antenna Array With Air Cavity Reflector for Integration in Plastic Packages," IEEE Antennas and Wireless Propagation Letters, vol. 11, 2012.

[11] S. Beer, C. Rusch, B. Gottel, H. Gulan, T. Zwick, M. Zwyssig, G. Kunkel, "A self-compensating 130-GHz wire bond interconnect with 13% bandwidth," IEEE International Symposium Antennas and Propagation Society (APSURSI), Orlando, FL, USA, July 2013.

[12] H. M. Rein and M. Möller, "Design considerations for very-high-speed Si-bipolar IC's operating up to 50Gb/s," IEEE J. Solid-State Circuits, vol. 31, no. 8, pp. 1076–1090, 1996.

[13] V. Valenta, W. Winkler, T. Spreng, D. Dancila, M. Kaynak, S. Yuan, A. Trasser, H. Schumacher, "High Performance Transmit/Receive Modules in 0.13 µm SiGe:C BiCMOS for Short Range F-band MIMO Radars," IEEE MTT-S International Microwave Symposium (IMS), Tampa, FL, USA, June 2014.

[14] N. Pohl, T. Jaeschke and K. Aufinger, "An Ultra-Wideband 80 GHz FMCW Radar System Using a SiGe Bipolar Transceiver Chip Stabilized by a Fractional-N PLL Synthesizer," IEEE Transactions on Microwave Theory and Techniques, vol. 60, no. 3, pp. 757-765, 2012.